Dynamic Clustering-based Model Reduction Scheme for Damping Control of Large Power Systems Using Series Compensators from Wide Area Signals

[*1]Soheil Ranjbar, [2]Ameena S. Al-Sumaiti, [3]Reza Sangrody, [4]Young-Ji Byon and [5,6]Mousa Marzband

[1]Electrical Engineering Department, Velayat University, Iranshahr, Iran.
[2]Advanced Power and Energy Center, Electrical Engineering and Computer Science Department, Khalifa University, Abu Dhabi 127788, UAE.
[3]Department of Electrical and Computer Engineering, Firoozkooh Branch, Islamic Azad University, Firoozkooh, Iran.
[4]CIEE, Khalifa University of Science and Technology, Abu Dhabi, UAE
[5]Northumbria University, Electrical Power and Control Systems Research Group, Ellison Place NE1 8ST, Newcastle Upon Tyne, UK
[6]Center of research excellence in renewable energy and power systems, King Abdulaziz University, Jeddah, Saudi Arabia.
*E-mail: s_ranjbar@sbu.ac.ir

***Abstract*—**This paper presents a new scheme of thyristor controlled series compensators (TCSC)-based damping controller for damping inter-area oscillations in bulk power systems based on a wide area measurement system (WAMS). In this regard, the proposed scheme provides an adaptive three-phase step through real-time working mode. In the first step, by proposing dynamic clustering-based technique, wide area signals evaluate the inter-area oscillations of the system which in a real-time procedure identify the corresponding oscillating areas. In the case of reducing the order of power systems through a set of aggregated coherent areas, the proposed scheme implements through the second step which utilizes as a damping controller for damping the inter-area oscillations. In this step, the wide area electromechanical signals use as input data through the proposed TCSC-based damping controller. The corresponding controlling signals consist of inter-area rotor angle ($\Delta\delta_{COI}$) and inter-area speed deviation ($\Delta\omega_{COI}$) evaluated through center of inertia (COI) frame. In the third step, at each time window (ΔT) through real-time working mode, the proposed scheme examines through a set of fault occurrences which based on online evaluations of the system dynamic responses, the controller parameters adjust adaptively. The proposed controller is an online and non-model-based scheme which properly reduces the system order through a set of coherent areas to provide proper damping performances of inter-area oscillations. The effectiveness of the proposed scheme evaluates through the Iran National Power Grid with the potential of two oscillating areas with proper damping performances for damping the unstable inter-area oscillations.

***Index Terms*—**Dynamic Clustering Technique, Damping Inter-Area Oscillation, Model Reduction, TCSC-based Wide Area Damping Controller.

1. Introduction

Evaluating large-scale power blackouts (i.e. blackout of 2003 at US Northeast) indicates unsecure performances of traditional model-based controllers compared to measurement-based controllers with respect to sever oscillatory conditions [1]. By using a wide area measurement-based technology namely WAMS within recent power systems, it is possible to measure the system dynamic signals with very fast sampling frequencies (i.e. 1024 sample/second) and evaluate the security-level of power system dynamics through different time durations [2]. **(R1-C1)** IEEE 1344, IRIG-B, and IEEE C37.118 are three useful standards which discuss the synchrophasor technology using PMU and GPS devices. In these standards, PMU is an electronic device which works based on synchrophasor technology to estimate the signal frequencies (up to 50/60 samples per cycle) using the voltage and/or current phasors. Based on the power system low frequency oscillations, PMUs can be very useful in light of the dynamic behavior of a power system to achieve wide-area monitoring, protection, and control. In this case of considering base frequency 60 Hz through test system and assuming sampling ratio 60 samples per cycles, there are 3600 samples per/sec can be extracted from PMU outputs. Based on the inter-area oscillation (IAO) frequencies in the range of 0.1-1 Hz, by selecting the highest IAO frequency f_{IAO}=1 Hz, the system time moving window Δt can be determined as $\Delta t=1/f_{IAO}$= 1 sec which is adequately enough to identify all IAOs. Therefore, a few numbers of PMU phasors (e.g. 10 point per/sec) is adequately enough to evaluate the IAO severity and determine proper control actions. As it is revealed, the number of PMU sampling ratio is not known as an important challenge through controller damping procedure.

Following the power network structure, WAMS-based measuring devices as Phasor Measurement Units (PMUs) are installed at multiple buses of the power system. Based on the PMUs technology and network configuration, different dynamical signals can be recorded and estimated with high sampling ratios.

Also, through using PMU-based signals, it is possible to develop primary protection systems which provide simpler actions for power network operators to take proper actions with respect to different contingencies. There are different real-time monitoring tools including US-Wide Frequency Monitoring Network (FNET) and Real Time Dynamics Monitoring System (RTDMS) [2] which are currently implemented throughout various locations of the US power network to monitor and evaluate the system frequency, current and voltage phasors.

Among various data analysis techniques and software principles, there are some outstanding algorithms or approaches targeting accurate identifications of behaviors of power system dynamics such as Prony analysis [3-4], sensitivity analysis [5-6], Hilbert-Huang transform [7-10] and phasor state estimation [11-15]. Recent literatures indicate that most of the provided techniques are concentrated on the use of synchrophasor

technology for the observation and monitoring of the power system. There are a few proper studies which have concentrated on examining and evaluating how the synchrophasor technology, instead of the traditional monitoring, can be implemented as an individual feedback controller. By progressing through measuring and controlling technologies, the use of wide-area control concept is attended within different power system studies especially on damping inter-area oscillations [1]. Evaluating the inter-area oscillations through several large-scale blackouts deducted that inter-area instability is a result of inadequate knowledge and improperly decided actions by the power network operators regarding minor events in the power system and thus leading to the large blackouts [16-20]. As an example, an unstable inter-area oscillation has occurred on August 10, 1996 through two coherent generator groups, one in Southern California and the other in Alberta. Such oscillations are against each other with a negative damping ratio. In this case, with respect to the lack of WAMS technology, the oscillations have not been observed by the operators and the magnitudes of oscillations have increased a time duration resulting in large blackouts that have occurred. Following this contingency, the US west grid has been separated into five uncontrolled islands [21].

Considering WAMS technology and corresponding identification techniques, it is possible to evaluate inter-area oscillations through a real-time working mode. For evaluating an unstable inter-area oscillation, considering some local and global damping controllers are attended to damp the oscillations [22].

In the case of damping controllers, the effectiveness of FACTS-based devices equipped with global signals as a wide-area damping controller has emerged during recent years. There are several methods that have been presented by power engineers over the past two decades to control power swings in tie-lines using TCSC-based controllers evaluated over different test systems [23-28].

Following different wide are damping control (WADC) schemes provided in the literatures, controlling multiple inter-area oscillations using a distributed wide-area damping controller (DWADC) remains as a research gap which has not been investigated deeply through WAMS-based technologies. Inspired from recognizing the issue, this paper addresses a generalized outlook of cluster-based techniques to present an adaptive wide-area damping controller equipped with TCSC compensators for damping different inter-area oscillations. Based on an inverse control strategy, the main idea is provided from which the proposed DWADC is designed. The proposed DWADC is an adaptive scheme to adjust controlling gains optimally with respect to oscillating patterns through online optimization techniques. With regards to the dynamic clustering technique, DWADC can be implemented through both reduced-order and higher-order power system cases. The most important innovations of the proposed DWADC scheme are developed through three following steps:

***Step1-Reducing the Model*:** In this step, considering wide area signals gathered from WAMS data followed by evaluating with the dynamic clustering technique, the reduced-order equivalent models of the power system are provided. In this case, the system synchronous generators are clustered through different coherent groups from which each group is modeled as an equivalent virtual generator (EVG) in the center of inertia (COI) frame. A typical power system consisting three EVGs and 8-tie-lines is illustrated in Figure 1.

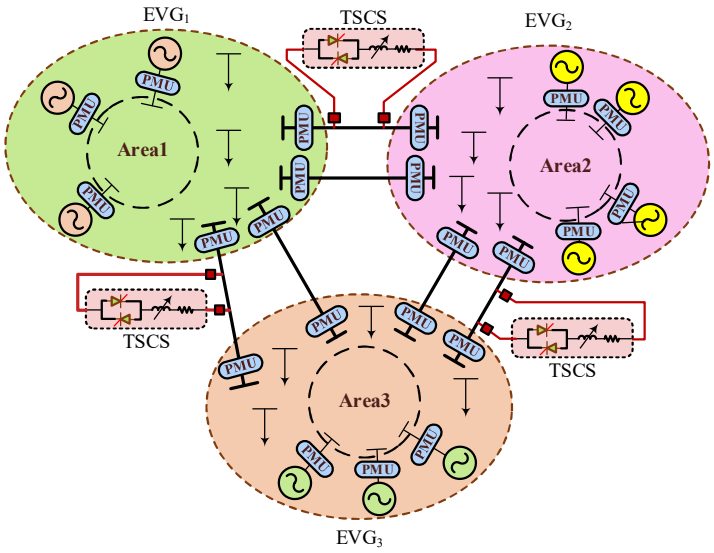

Figure 1: Typical test system with three coherent groups and controlled TCSCs for damping the oscillation.

From Figure 1, depending on the generators' inertias, the provided EVGs consist of different inertias HEVGi and oscillation behaviors that are connected through several tie-lines. Based on the coherency concept through the COI frame, the system is divided into three coherent equivalent groups as EVG_1, EVG_2 and EVG_3. In the case of identifying coherent groups and corresponding tie-lines, the proposed DWADCs are provided. Depending on the oscillating areas, DWADCs are connected through different tie-lines. Detailed explanations related to identifying coherent groups and modeling EVGs have been presented in our previous work in [1] which had focused on modeling and damping inter-area oscillations.

***Step2-Aggregation*:** In this step, the required online procedure related to the proposed TCSC-based DWADC scheme is provided. In order to implement the proposed scheme, a modal analysis is conducted and inter-area oscillating patterns are analyzed from which DWADC parameters are adjusted. By using the online optimization technique and monitoring DWAC damping performances, the parameters are evaluated online from which the values with the best damping ratios are considered as DWADC controlling parameters.

***Step3-Inversion*:** This step evaluates the proposed DWADC scheme with a realistic full-order test system setup. Considering damping controllers installed at candidate tie-lines, comparative studies of damping performances of DWADCs with reduced-order and practical full-order system are evaluated. Inspired from this

issue, a DWADC scheme developed for the reduced-order EVGs are redesigned for realistic test-system considering similar modal analysis procedures. The DWADC parameters are evaluated to reach proper damping performances with respect to a full-order test system.

By considering online evaluations, the abovementioned three-step approach can be implemented properly on a *n*-area power system consisting of different oscillating patterns from which the proposed DWADC scheme can be considered as a suitable choice to solve the inter-area damping issues in the presence of multiple oscillating areas.

This paper is organized as in the following. In Section 2, by considering *n*-machine power system, a TCSC-based DWADC is formulated through a set of optimization problems. In Section 3, based on evaluating wide area signals gathered from WAMS data, the proposed dynamic clustering technique to reduce the system order is developed. In Section 4, following the Model Reference Control (MRC) technique, the inversion of two-area power systems into an actual full-order power system is provided which is evaluated through simulation results. Finally, Section 5 presents the main conclusions of the paper and its innovative contributions to the field.

2. Mathematical formulation of DWADC scheme for *n*-area power system

In this section the required formulations for a *n*-area power system is provided. Considering various relevant factors including a power system with n_G generator buses, n_T transmission buses (also addressed to zero injection buses) and n_L load buses, the mathematical problems are developed. In the case of n_l buses, considering a set of nominate loads consisting of both active and reactive powers, the load buses are determined. Also, in the case of transmission buses n_T and following the load flow constraints, the input powers forming one side of the n_T buses (i.e. consists of both active and reactive power) are equal to the output powers from the other side of the buses. Based on this, considering power system with total buses $n= n_G+ n_L+ n_T$, the active P_i and reactive Q_i powers of ith individual bus provided by load flow calculations are defined as follows:

$$P_i^N = \sum_{k-1}^{n} \left(\frac{V_i^2 r_{ik}}{y_{ik}^2} + \frac{V_i V_k \sin(\delta_i - \delta_k - \alpha_{ik})}{y_{ik}} \right) \tag{1}$$

$$Q_i^N = \sum_{k-1}^{n} \left(s\frac{V_i^2 x_{ik}}{y_{ik}^2} + \frac{V_i V_k \cos(\delta_i - \delta_k - \alpha_{ik})}{y_{ik}} \right) \tag{2}$$

where, δ_i and V_i are the voltage angle and magnitude of ith buses, respectively.

In (1) and (2), α_{ik} and y_{ik} are the reactance and resistance of the line, connected through the k^{th} and i^{th} bus, respectively.

$$\alpha_{ik} = \tan^{-1}(r_{ik} / x_{ik}) \tag{3}$$

$$y_{ik} = \sqrt{r_{ik}^2 + x_{ik}^2} \tag{4}$$

Considering three types of buses, the provided variables V_i, δ_i, P_i^N, Q_i^N are defined as load variables (V_L, δ_L, P_L^N, Q_L^N), transmission variables (V_T, δ_T, P_T^N, Q_T^N) and generator variables (V_G, δ_G, P_G^N, Q_G^N) corresponding to the three buses n_L, n_T and n_G, respectively. In (1) and (2), the generator's voltage magnitudes V_G at generator buses are adjusted through the feedback control strategy such that the frequencies f_G and bus angles δ_G are two dynamic variables of n_G buses. Therefore, the dynamic model of the power system consists of electromechanical variables that can be described through differential-algebraic equations (DAE) given as follows.

$$\dot{\delta} = \omega \tag{5}$$

$$\left(M_g \dot{\omega}\right) = P_G^E + P_G^N - \left(D_G \times \omega\right) \tag{6}$$

$$Q_T^N = P_T^N = 0 \tag{7}$$

where,

ω represents the generators' speed deviation with respect to a reference machine ω_0.

M is the synchronous generator's inertias within $n_G \times n_G$ dimensional diagonal matrix which is equal to $M_i=2H_i$ with respect to ith synchronous machine.

D_G is the damping factor of generators within $n_G \times n_G$ dimensional diagonal matrix.

P^E_G represents the corresponding active power injected the system from generator buses.

(R2-C1) It should be noted that, the proposed reduced-order procedure is concentrated through damping the inter-area oscillations. To do this, by using the simplified 2th order model of synchronous generators consisting of rotor angle and speed variables, the system coherent groups and corresponding equivalent virtual generators (EVGs) are provided. Automatic voltage regulator (AVR) has significant effects through adjusting the generators internal voltage and improving theirs transient stabilities. Through conventional models, AVR adds a set of eigenvalues through the system in the range of 0-0.1 Hz which provide synchronous torques to control the local oscillations and transient conditions. However, the aim of this paper is mainly concentrated through damping inter-area oscillation in the frequency range of 0.1-1 Hz which is out of range of AVR controlling boundaries. Therefore, by simplifying the generator order and identifying the coherent generators as one virtual generator, the whole of power system is modeled through a set of EVGs which are oscillating against each

other. In this case, by using the proposed WADC scheme connected between the oscillating areas, the controlling parameters with positive effects through damping inter-area oscillations are provided.

Considering the steady state condition, the generator's electrical power output P^{E}_{G} are equal to the mechanical input power P_m to the generators.

In (5)-(7), adopting the Kron reduction-order technique [23], the provided DAE orders can be decreased to a reduced-order differential model that consists of only the main dynamic variables. In this case, the reduced-order power system is described as a graph-based network with n_G generators (nodes) connected together through m tie-lines, where $m \leq n(n\text{-}1)/2$. Based on this, the power system is modeled with a graph-based theory. Graph=(ν,ε) consists of v nodes and ε edges connected through $n \times m$ connections. The tie-lines are connected together through connection links such that the arrows indicate the direction of efficient power flows. Considering the synchronous machine theory, $E_i=|E_i|\angle \delta_i$ is the polar form of the internal voltage phasor from the ith generator. δ_i represents the generator's rotor angle and $|E_i|$ is the generator's internal voltage magnitude. Also, in order to make the transmission lines connecting the ith and jth generators to be lossless, the reactance between two synchronous machines can be developed as follows:

$$\tilde{x}_{ij} = x'_{d,i} - x'_{d,j} - x_{ij} + \Delta x_{ij}(t) =: \tilde{x}_{ij} + \Delta x_{ij}(t) \tag{8}$$

where $x'_{d,i}$ and $x'_{d,j}$ indicate the transient reactance of the ith and jth generator in the direct-axis component, $x_{ij}>0$ is the constant tie-line reactance through the ith and jth generator, and $\Delta x_{ij}(t)$ is an available tie-line reactance, which can be modified by TCSC. Also, $\tilde{x}_{ij}$ indicates the total reactance through the ith and jth generators.

Considering the provided reactance model (8), $i \in N_i$ and $i \in \{1,2,\ldots,n\}$, N_i presents the controlling nodes through the ith generator's node connections. It is worth noting that, in the case of identifying TCSC locations, considering three oscillating areas as shown in Figure 1, the corresponding tie-lines are aggregated together through $\beta \subset \varepsilon$ links that one TCSC is connected between oscillating areas. In this case, there are m tie-line connection links which are connected within i and j generator machines. Based on this, a corresponding graph-based theory is developed. By considering the ith and jth synchronous generators, there is a set of edges ε_{ij} which connects generators' nodes together. Based on the tie-line reactance and considering $x_{ij}=x_{ji}$, the mathematical formulation (8) can be used to find a weighted factor of the power network for adopting the graph-based theory. In case of two nominated nodes not having any line connections, the corresponding reactance for a non-existing edge is set to an infinite value (i.e., open circuit) or $y_{ij} = 1/x_{ij} = 0 \ \forall j \notin N_i$.

Similarly, in the case of $\varepsilon_{ij} \notin \beta$, the corresponding reactance $\Delta x_{ij}(t)$ goes to zero ($\Delta x_{ij}(t) = 0$). In this case, the tie-line reactance x_{ij} and the corresponding edges ε_{ij}, which are not equipped with DWADC controllers, are not performed during the damping control procedure and the corresponding available reactance $\Delta x_{ij}(t)$ is fixed when monitoring the damping performance of the TSCS controller.

By ignoring the generators' damping factors D_G, the developed DAE electromechanical models (5)-(7) of the ith synchronous generator, considering the first-order model of TCSC controller, can be described as follows [8].

$$\dot{\delta} = \omega_i - \omega_N \tag{9}$$

$$2H_i \dot{\omega}_i = P_{mi} - \sum_{k \in N_i} \frac{E_i E_k \sin(\delta_i - \delta_k)}{\tilde{x}_{ik} + \Delta x_{ik}(t)} \tag{10}$$

$$\Delta \dot{x}_{ij} = -\frac{1}{T_{ij}} \Delta x_{ij} + u, \quad \forall e_{ij} \in \beta \tag{11}$$

where ω_i and ω_N are the rotor speed and synchronous speed with respect to a base frequency of 60 Hz, respectively. T_{ij} is the time-constant of the TCSC dynamic response installed through the tie-line ij, and u represents the controlling signals developed as input wide-area signals for the TCSC-based DWADC scheme.

All of the developed dynamic variables are in per unit scales of which only the phase angles are defined in radians. Following the dynamic formulations (9)-(11), the power network configuration is evaluated. Dynamic variables and available reactance are evaluated considering N_i buses through i=1, 2, …, n. In this case, considering initial equilibrium points (δ_{i0},0) where $0 < \delta_0 < 90$ for all i=1, 2, …, n, the mentioned dynamic variables (9)-(11) are evaluated as follows:

$$\Delta\delta = col(\Delta\delta_1, \Delta\delta_2, ..., \Delta\delta_n) \tag{12}$$

$$\Delta\omega = col(\Delta\omega_1, \Delta\omega_2, ..., \Delta\omega_n) \tag{13}$$

$$\Delta x = col(\Delta x_1, \Delta x_2, ..., \Delta x_l) \quad \forall e_{pq} \in \beta \tag{14}$$

where, the l index through reactance parameter Δx develops the size of tie-lines through the variable set β.

Considering behaviors of the TCSC dynamics with respect to an inter-area oscillation frequency, the dynamic state variables (9)–(11) can be described in form of steady-state linearized dynamic formulations shown as follows:

$$\begin{bmatrix} \dot{\Delta\delta} \\ \dot{\Delta\omega} \\ \dot{\Delta x} \end{bmatrix} = \underbrace{\begin{bmatrix} 0 & I_n & 0 \\ M^{-1}L & 0 & M^{-1}g \\ 0 & 0 & -D \end{bmatrix}}_{A} \begin{bmatrix} \Delta\delta \\ \Delta\omega \\ \Delta x \end{bmatrix} + \underbrace{\begin{bmatrix} 0 \\ 0 \\ I_l \end{bmatrix}}_{B} u \tag{15}$$

In (15), M=diag(M_1, M_2, …, M_i), n and l are the system matrix dimensions with respect to the identity parameters I_n and I_l, respectively. In this case, the system damping factor D is ordered to $1/T_{ij}$ for all $\varepsilon_{ij} \in \beta$. Also, zero values are set to present the initial conditions of the dynamic state variables. From (15), the parameter L represents the system Laplacian functions within $n \times m$ dimensional matrices as follows:

$$L_{nm} = -\sum_{k \in N_n} \frac{E_n E_m}{\bar{x}_{nk} + \Delta x_{nk}(t_0)} \cos(\delta_{n0} - \delta_{k0}) \tag{16}$$

$$L_{nk} = \frac{E_n E_k}{\bar{x}_{nk} + \Delta x_{nk}(t_0)} \cos(\delta_{n0} - \delta_{n0}) \quad k \in N_n \tag{17}$$

$$L_{nk} = 0, \ otherwise \tag{18}$$

In the case of M_i=M_j , the provided Laplacian matrix L_{nm} is represented with transported form as L=L^T.

Considering a bulk power system, there are various synchronous generators within different inertias H_i resulting in unsymmetrical Laplacian function L_{nm}. Following the developed dynamic variables (15), the corresponding function $M^{-1}L$ is defined as an unsymmetrical matrix through swing equations. From (15), it is concluded that depending on the inter-area oscillation patterns, there are a set of dynamic variables (i.e. synchronous generators) which are coherent with each other. Depending on the generators' correlation coefficients, there are different oscillating areas with the potential of unstable inter-area oscillations according to the severity of fault events. For the controlled separating scenario, the oscillating areas and the corresponding boundary nodes are specified through different cluster groups, adopting the graph-based theory. The developed Laplacian matrix L is reorganized as a block matrix that consists of small oblique matrixes which indicate the system coherent groups connected through links. Also, in the case of two areas i and j that are specified as one coherent group, the corresponding oblique matrixes B_{ij} goes to the lowermost row through the rightmost component to be non-zero so that all other arrivals are zero.

The corresponding non-zero arrivals present the inter-area oscillating areas, which can be used to reduce the order of main system through reduced-order model. The reduced-order model only develops the system dynamic state variables which can be evaluated through identification schemes as in the variable identification rules presented in [29]. Considering the TSCS-DWADC scheme to control the tie-line reactance Δx_{ij}, the

reduced-order model (15) develops the system-dynamics behaviors in the form of a rotor angle $\Delta\delta$ and a speed $\Delta\omega$ deviations. Therefore, considering the linearized dynamic formulation (10), the speed deviations dynamic state variable $\Delta\omega$ can be described as a function of the tie-line reactance $\Delta x(t)$ as follows:

$$M_n \dot{\Delta\omega}_n = -\underbrace{\sum_{k\in N_n} \frac{E_n E_k \sin(\delta_{n0}-\delta_{k0})}{(x_{nk}+\Delta x_{nk}(t_0))^2}}_{\xi_{nk}} \Delta x_{nk}(t) - v(\Delta\delta_n, \Delta\delta_k) \tag{19}$$

where, the second part of (19), $v(\Delta\delta_n, \Delta\delta_k)$ is a function of rotor angle oscillations with $\Delta x(t)$ dependency.

Considering the first part of (19), the DWADC input signals can be deducted from an organized list through parameters ζ_{nk} with respect to each variable $\varepsilon_{ij} \in \beta$. Depending on the provided model, the input signals for the Δx dynamic state variable is ordered.

In this case, following the developed coherent groups, the corresponding TCSCs are located through tie-lines connecting links between two oscillating areas. A more realistic power system test case with a potential of three coherent areas is presented in Figure 2. From Figure 2, the power system has the potential of three oscillating areas (Area1, Area2 and Area3). By identifying the corresponding tie-lines, TCSC-based DWADCs are located through oscillating areas as shown in Figure 2.

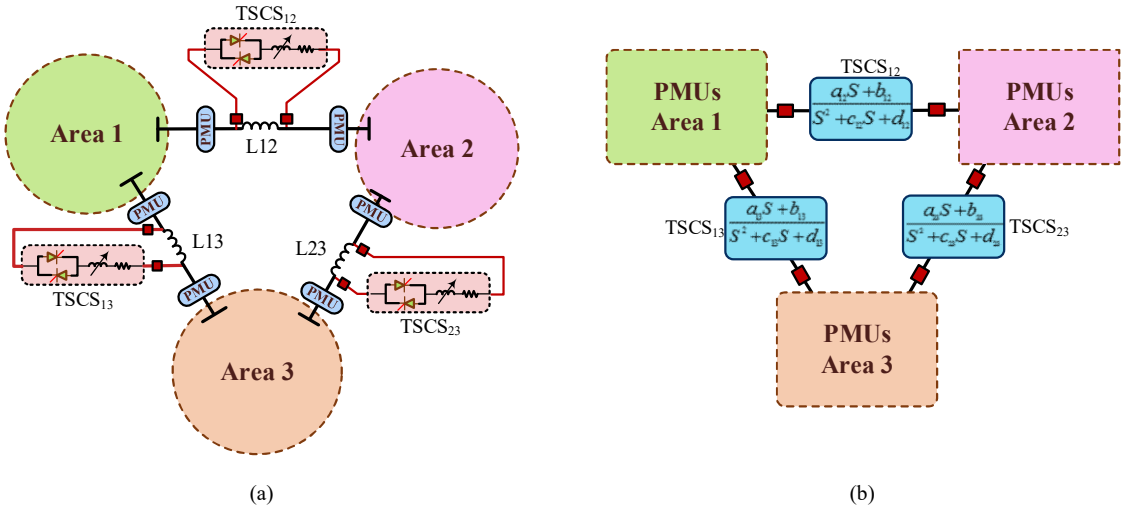

(a) (b)

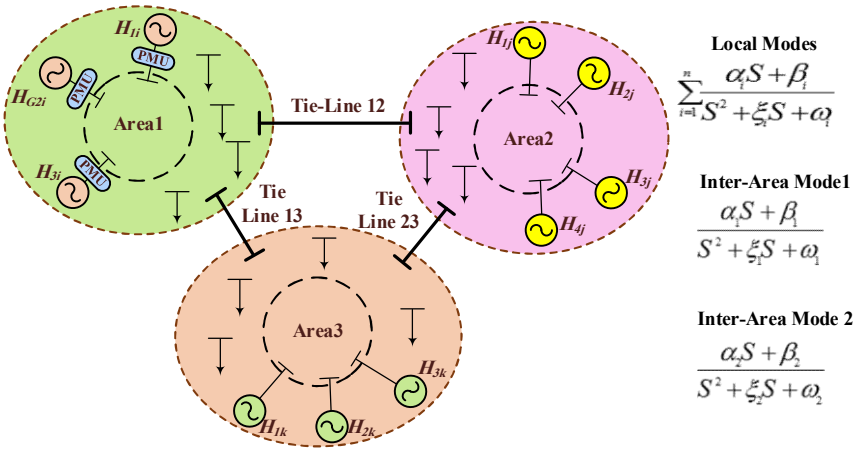

(c)

Figure 2: Power system with three oscillating areas equipped with TCSC-based DWADCs connected through inter-area tie-lines. (a) TSCSs located through identified tie-lines, (b) Controlling diagram, (c) Reducing the model order according to coherent generators and inter-area modes.

Based on the concept of correlation coefficient for generators, the power system can be simplified through three oscillating areas. Each area consists of aggregated generators. It is worth noting that, through a reduction in the power-system order, the tie-lines and the corresponding TCSCs are fixed such that the generator dynamic variables and interconnection links are simplified. In this case, following the linearized state-feedback classical control scheme, the proposed DWADC scheme is provided. The system damping performances are evaluated considering TCSC-based controllers through oscillating areas. The proposed DWADC scheme that consists of the generalized control concept is developed as a reference model for which the input-signal gains and time constancies are adjusted optimally depending on the system damping responses with respect to experienced inter-area oscillations.

Solving this issue, the DWADC parameters are optimized following an online optimization procedure. Based on Figure 2, the swing equation of the *j*th reduced-order EVG consists of a damping factor d_j that is described as follows:

$$\frac{d}{dt}\left(\delta_j\right)=\omega_j \tag{20}$$

$$M_j\frac{d}{dt}\left(\omega_j\right)-\left(d_j\right)\omega_j-P_{mj}-P_{ej}\left(\delta,\Delta x\left(t\right)\right) \tag{21}$$

where, P_{ej} is the electrical output power of *j*th generator, and $\Delta x(t)$ represents state variables of the TCSC controller.

Also, from Figure 2, it can be seen that power system is equipped with a set of PMU devices at different locations. Considering the PMU signals and the corresponding gains defined as y_j and k_j respectively, the

available measuring devices of *j*th EVG utilized as feedback signals can be developed in a form shown in the following:

$$(y_1^{j1},k_{j11}),\,(y_2^{j1},k_{j21})\,...,(y_1^{j2},k_{j12}),...,(y_m^{jm},k_{jmn}) \tag{22}$$

where y_j indicates the *j*th available signal measured by the *j*th PMU device. Also, index j_m presents the bus location *m* near the *j*th synchronous generator through reduced-order model.

PMUs present the current and voltage phasors within high sampling ratios (i.e. 1024 sample/sec). In this case, the available signals extracted from PMU phasors can be provided via the current and voltage magnitudes, current and voltage angles, active and reactive powers, apparent impedances, and the system electrical frequency. Following the signal specifications (22), PMU measurements can be used as wide-area input signals to the TSCS-based DWADC scheme. A typical design of an output feedback structure as input wide-area signals using the reduced-order model can be explained as follows:

$$u_j - f(y_1^{j1}(t),\, y_2^{j1}(t),\, ...,\, y_m^{j_n}(t), k_{j11}, k_{j21}, ..., k_{jmn}) \tag{23}$$

The second part of (23) is a function of PMU signals, which provides the power system transient responses. It is worth noting that for providing the same damping performances, the parameter u_i is modified depending on the system full-order and reduced-order model. To do this, defining a nonlinear variable ρ, the feedback controlling gains (k_{j11}, k_{j21}, ... , k_{jmn}) of DWADCs connected between oscillating areas are evaluated. Considering *l* as the number of coherent generators through the *j*th area, and parameters k_{jmin} and ρ^l_{min} as two corresponding constraints, the state variables *k* and *R* through (*j*,*l*,*m*,*n*) dimension can be solved as an objective function (OF) as given below:

$$OF = \min\left(x_{ij}(t,\Re(\kappa)) - \bar{x}_{ij}(t,\kappa)\right)^2 < e \tag{24}$$

where, x_{ij} and $\bar{x}_{ij}$ represent the full-order model and the reduced-order model dynamic responses with respect to inter-area mode specifications (i.e. frequency or phase) between two oscillating areas *i* and *j* respectively.

k represents a set of constraints that consist of the lower and upper boundaries for developing feedback signal gains.

Considering the error *e* as a dynamic response difference between two specified models, the objective function (24) is evaluated by following an optimization procedure from which the best reduced-order model is provided. In the case of the oscillations of two or three inter-area modes occurring on the test system, there are a set of non-individual constraints bounding the optimization problem (24) with respect to candidate inter-area

modes, for which the reduced-order model is applied. Power system consisting of two inter-area modes and corresponding oscillating areas are illustrated in Figure 2(c). Based on Figure 2(c), in the case of PMU signals are included with two or three oscillating modes, considering decomposition techniques such as Eigenvalue Realization Algorithm (ERA) [30], Prony analysis [4], etc., an inter-area mode with the most important frequencies and gains are identified and extracted from evaluated signals. Considering the most important inter-area modes, a dynamic equivalent circuit of reduced-order model is developed.

It is worth noting that depending on the candidate inter-area modes, there are different reduced-order models with different frequencies that are used for controlling the specified oscillating modes. From Figure 2(c), considering the test system with both inter-area and local modes, the full-order transfer function of the test system can be written in the form of pole residues described as follows:

$$G(s)=\underbrace{\sum_{i\in N_l}\frac{\sigma_i s+\mu_i}{s^2+\gamma_i s+\pi_i}}_{Local\ Modes}+\underbrace{\sum_{p}\left(\frac{\mu_p}{s+\pi_p}\right)^n}_{TCSC-based\ DAWDC\ Model}+\underbrace{\sum_{j,k\subset N_j\times N_k}\frac{\sigma_{jk}s+\mu_{jk}}{s^2+\gamma_{jk}s+\eta}}_{Inter-Area\ Modes} \tag{25}$$

where N_l presents the number of local modes and $N_j \times N_k$ develops the number of inter-area modes through oscillating areas i and j, respectively.

Since, inter-area mode specifications (σ_{jk} , μ_{jk}) are not equal at the different oscillating modes, their evaluated PMU signals are included with different participation factors of the inter-area modes. Therefore, depending on the candidate inter-area mode, the estimated clusters and the corresponding reduced-order models are different. In order to evaluate DWADC specifications (25), considering the jth inter-area mode, the corresponding DWADC model is provided, which is designed to control the candidate mode. Therefore, for controlling all possible inter-area oscillations, there are M DWADCs which are optimized individually with respect to oscillation frequencies and damping ratios when considering M inter-area modes. In this case, three following remarks should be attended.

Remark 1: By following the dynamic state variables (9)–(11), it is possible to design different DWADCs through tie-lines considering the objective functions (24) and (25), from which a reduced-order model and corresponding DWADC specifications can be found. In this paper, depending on the number of oscillating areas, DWADCs are designed and developed through corresponding tie-lines. In this case, buses equipped with long transmission-lines can be specified as candidate DWADC buses.

(R1-C3)*Remark 2*: *A* design procedure of the proposed DWADC scheme is provided similar to the conventional Power System Stabilizers (PSSs) which is optimized to damp both the local and inter-area

oscillations. It should be noted that through developed scheme, the synchronous generators are equipped with local PSSs which are responsible for damping the local modes with respect each individual generator inertia parameters. In this case, the proposed WADC controller is concentrated to damp the unstable inter-area oscillations which by using the inter-area rotor angle ($\Delta\delta_{COI}$) and speed deviation ($\Delta\omega_{COI}$) in COI frame as input signals, the determined inter-area modes are controlled.

(R2-C2)*Remark 3:* For real-time estimations of the generators rotor angles, there are several analytical methods in literature (e.g. Ref.[1], [4], [5],…) which are concentrated through estimating rotor angle deviations of synchronous generators. In this regard, all of the generator buses are equipped with phasor measurement units (PMU) which sent the measured signals through some communication links. Regarding to communication link type, signals are transmitted within different latencies which must be compensated to provide proper damping performance. In this study, developing a pade approximation method [16], delays are estimated from which regarding to adaptive first order compensation blocks, the existed delays are compensated.

3. Identifying oscillating areas using dynamic cluster technique based on PMU data

This section provides an Inter-area Model Estimation (IME) technique for identifying oscillating areas with coherent generators. To do this, considering wide area signals gathered from PMU data, the reduced-order model is provided which can be applied for multi-area power systems. A typical reduced-order power system consists of two oscillating areas (Area 1 and Area 2) as presented in Figure 3. From Figure 3, *EVG1* and *EVG2* represent the equally reduced-order model of the two oscillating areas. The two inter-area buses *B1* and *B2* of Area 1 and Area 2 are the two points connecting the areas via the long transmission line X_e. In this case, both virtual generators *EVG1* and *EVG2* consist of several coherent synchronous machines which can be looked at as one virtual generator through the reduced-order model. Voltage phasors of two equivalent generators consist of amplitudes and phase angles and can be described as $E_{EVG1}=|E_{EVG1}|\angle\delta_{EVG1}$ and $E_{EVG2}=|E_{EVG2}|\angle\delta_{EVG2}$, which oscillate through two virtual inertias H_{EVG1} and H_{EVG2}, respectively. From Figure 3, the reactance $jx_{i\text{-}j}$ presents the interconnected line reactance through each $Area_i$ which in the case of generator buses, is merged with the generator's transient reactance $x`_d$ and the corresponding transformer reactance x_T in a unit value. Power flow calculations between the two inter-area Buses *B1* and *B2* (considering a third middle bus as Bus 3, as shown in Figure 3), illustrate that by following the occurrences of small signal faults through the tie-line, it is possible to identify that the system has a potential of inter-area oscillation through two oscillating areas *Area1* and *Area2* which can be evaluated by voltage amplitudes V_1, V_2, V_3 and the corresponding phase angles θ_1, θ_2, θ_3.

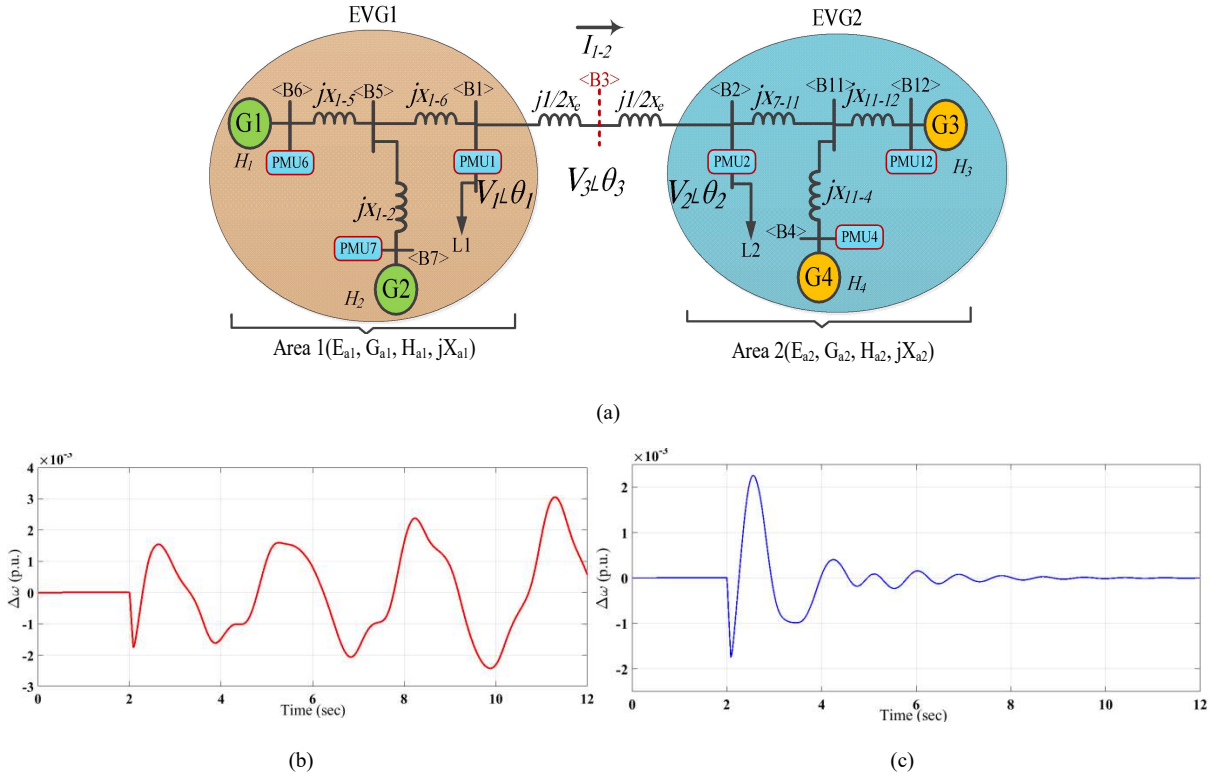

Figure 3: Estimating two-area test system and system dynamic performance through with respect to two stable and unstable cases.

(a)Estimating inter-area model for a two-area test system, (b) Unstable case, (c) Stable case.

Based on Figure 3(a), following the wide area signals measured from PMU data and considering the developed IME technique, the two provided oscillating areas are estimated through the dynamic state variables as x_{EVG1}, x_{EVG2}, H_{EVG1} and H_{EVG2} in a form of the reduced-order model. In this case, considering the generator's internal reactance jx, the voltage magnitude and the corresponding phase angle evaluated from the generator's buses are provided as follows:

$$\tilde{V} = \underbrace{\left(\frac{x}{(x_{EVG1}+x_{EVG2}+x_e)}\right)}_{r} \times \left(E_1\cos(\delta) - E_2 + jE_1\sin(\delta)\right) + E_2 \tag{26}$$

From (26), considering $r=x/[x_{EVG1}+x_{EVG2}+x_e]$, the voltage phase angle is derived as:

$$\theta = \tan^{-1}\left(\frac{rE_1\sin(\delta)}{rE_1\cos(\delta)+(1-r)E_2}\right) \tag{27}$$

Based on a small-signal stability concept, following few changes (27) against angle δ, the phase angle deviation $\Delta\theta$ can be rewritten as follows:

$$\begin{aligned}\Delta\theta(r,t) &= \frac{\partial}{\partial\delta}\left[\tan^{-1}\left(\frac{rE_1\sin(\delta)}{rE_1\cos(\delta)+(1-r)E_2}\right)\right]\Delta\delta(t) \\ &= \left(\left[\frac{r^2E_1^2 + r(1-r)E_1E_2\cos(\delta_0)}{r^2E_1^2}\right] + \left[(1-r)^2E_2^2\right] + \left[2r(1-r)E_1E_2\cos(\delta_0)\right]\right)\Delta\delta(t)\end{aligned} \tag{28}$$

From (28), the parameters E_1, E_2 and δ_0 can be substituted with the following descriptions

$$E_1 = |\tilde{V}_1 + jx_{EVG1}\tilde{I}| \tag{29}$$

$$E_2 = |\tilde{V}_2 - jx_{EVG2}\tilde{I}| \tag{30}$$

$$\delta_0 = \angle(\tilde{V}_1(0) + jx_{EVG1}\tilde{I}(0)) - \angle(\tilde{V}_2(0) + jx_{EVG2}\tilde{I}(0)) \tag{31}$$

where, $\tilde{V}_1(t)$, $\tilde{V}_2(t)$ and $\tilde{I}(t)$ represent the system-wide area signals evaluated from the PMU data with respect to each time window Δt.

By substituting (29)-(31) into (28), the provided phase angle deviation $\Delta\theta$ is simplified such that the areas' reactance x_{EVG1} and x_{EVG2} are the only two unknown variables in the provided model. In this case, considering the two following algebraic differential formulations, the phase angle $\Delta\theta$ is calculated.

$$\frac{\Delta\theta(r_1,\bar{t})}{\Delta\theta(r_2,\bar{t})} = \frac{\varsigma(r_1,E_1,E_2,\delta_0)}{\varsigma(r_2,E_1,E_2,\delta_0)} \tag{32}$$

$$\frac{\Delta\theta(r_3,\bar{t})}{\Delta\theta(r_2,\bar{t})} = \frac{\varsigma(r_3,E_1,E_2,\delta_0)}{\varsigma(r_2,E_1,E_2,\delta_0)} \tag{33}$$

where, $\Delta\theta(r_1,\bar{t})$ represents the phase angle deviation evaluated from the ith PMU_i device through the time window Δt with respect to the provided equilibrium point.

Considering (32) and (33), the internal variables r_1, r_2 and r_3 are provided as follows:

$$r_1 = \frac{x_{EVG2} + x_e}{x_{EVG1} + x_{EVG2} + x_e} \tag{34}$$

$$r_2 = \frac{x_{EVG2}}{x_{EVG1} + x_{EVG2} + x_e} \tag{35}$$

$$r_3 = \frac{x_{EVG2} + 0.5x_e}{x_{EVG1} + x_{EVG2} + x_e} \tag{36}$$

Regarding the area inertias, the following frequency extrapolations through the three corresponding buses and the area equivalent inertias H_{EVG1} and H_{EVG2} are calculated.

Considering the provided dynamic formulation (9), the linearized swing equation for two oscillating areas with virtual generators EVG_1 and EVG_2 can be written as follows:

$$\Delta\delta(t) = \alpha_1 \cos(mt) + \alpha_2 \sin(mt) \tag{37}$$

where, $\alpha_1=\Delta\delta(0)$, $\alpha_2=\Delta\omega(0)$ and $m=E_1E_2\cos(\delta_0)/x_e$.

Finally, by substituting the rotor's angle deviation (37) into the phase angle deviation (28), the corresponding phase angle deviation $\Delta\theta$ of the virtual generators through dynamic state variable is provided as follows.

$$\Delta\theta(r,t) = \left(\left[\frac{r^2E_1^2 + r(1-r)E_1E_2\cos(\delta_0)}{r^2E_1^2} \right] + \left[(1-r)^2E_2^2 \right] + \left[2r(1-r)E_1E_2\cos(\delta_0) \right] \right) \times (\alpha_1 \cos(mt) + \alpha_2 \sin(mt)) \tag{38}$$

It is worth noting that the provided phase angle deviation $\Delta\theta$ consists of two reactance-based (r) and time-based (t) individual parts, which can be separated as two different variables as follows:

$$\Delta\theta(r,t) = \Delta\theta_a(r) \times \Delta\theta_b(t) \tag{39}$$

(R1-C4) From (39), $\alpha_1=\Delta\delta(0)$, $\alpha_1=\Delta\omega(0)$, $m=E_1E_2\cos(\delta_0)/x_e$, $r=x/[x_{EVG1}+x_{EVG2}+x_e]$, and t is the time duration. As, it can be seen, based on the system operational and topological conditions evaluated from WAMS data, the variable values can be determined. In order to validate the proposed reduced-order function (39), considering a set of arbitrary values within limited boundaries, the proposed function effectiveness is evaluated. In this case, considering some typical parameters as m=1, α_1=1, α_2=0.1, r=[0,1] and t=[0,15], the EVG dynamic oscillations are evaluated. Rotor speed oscillations with respect to the two stable and unstable cases are presented in Figure 3(b, c). As it can be seen in Figure 3(c), in the case of considering the damping factor parameter D through the provided dynamic state variables, the rotor angle dynamic oscillations evaluated from (37) will be damped through the specified time duration.

From Figure 3(b), it is illustrated that depending on the system damping parameter, the provided EVG presents different dynamic behaviors consisting of different damping ratios. In this case, both the denominator and nominator parameters will be impacted through the dynamic oscillations and corresponding damping ratios. From the evaluated formulation (37) and the provided simulation results, it is concluded that the order of power system is properly reduced so that the reduced-order model develops proper dynamic responses with respect to the fault event scenario. It is worth noting that the provided model parameters are dependent on the system operating conditions. With respect to system operating points, it is found that they have some dynamic oscillations during the time window Δt.

4. TCSC-based DWADC controlling model

In this section, considering a power system with the potential of two oscillating areas, the required procedure for developing DWADC controlling model is provided. Based on Figure 4, evaluating the measuring data through modal analysis technique showed that the power system has a potential of inter-area oscillation between two oscillating areas (*Area1* and *Area2*). In this case, the reduced-order model equipped with one participation factor presents the inter-area mode specifications. Considering a specified oscillating mode, the reduced-order model is provided for which the corresponding DWADC controlling model is designed. Figure 4 presents a typical power system with two oscillating areas equipped with the TSCS-based WADC through a tie-line communication link. From Figure 4, buses *B1* and *B2* indicate the candidate *EVG* buses through the provided equivalent generators and TCSC link.

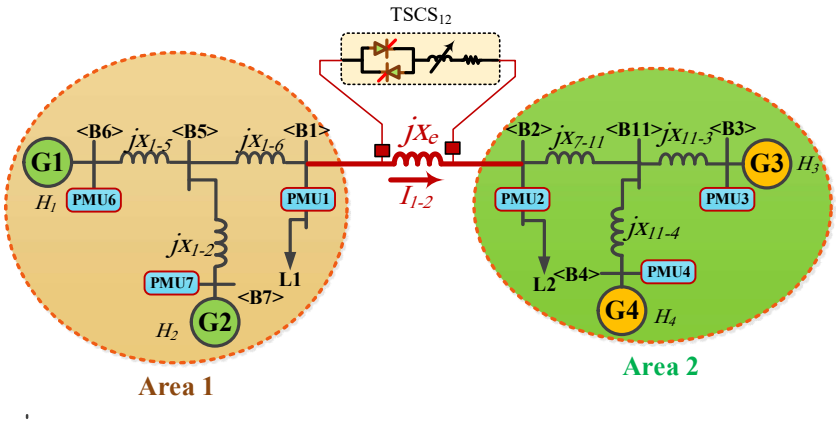

Figure 4: The equivalent two-area power system with a TCSC controlling link.

As previously presented in Sec.1, the provided MRC controlling model can be performed as an efficient technique for inversing the controlling model through the simplified Laplacian states. In this case, considering the following lemma and the generic optimization technique provided in Sec.2, the required procedure for optimizing and simplifying the controlling model is developed.

Lemma1: The mathematical formulation (25) is considered as a controlling model of the generator's transfer functions of *EVG*(*s*) and TCSC link through the provided virtual generators. In this case, following phase angle deviations through two inter-area buses *B1* and *B2*, different controlling behaviors can be found. It is noted that, depending on the inter-area oscillation frequency, the corresponding DWADC controlling order *n* is estimated.

Proof: Considering the rotor's phase angle δ and the speed deviations ω as the main dynamic state variables, the corresponding swing equations are redefined as follows:

$$\delta = \begin{matrix} col\,(\delta_{11},\delta_{12},...,\delta_{1n_1}) \\ col\,(\delta_{21},\delta_{22},...,\delta_{2n_2}) \end{matrix} \tag{40}$$

$$\omega = \begin{matrix} col\,(\omega_{11}, \omega_{12}, ..., \omega_{1n_1}) \\ col\,(\omega_{21}, \omega_{22}, ..., \omega_{2n_2}) \end{matrix} \tag{41}$$

where δ_{ij} and ω_{ij} represent the rotor angle and speed deviations of jth synchronous machine with respect to ith oscillating area, respectively. Also, n_1 and n_2 represent the total number of synchronous machines operating through the two oscillating areas (*Area1* and *Area2*).

In this case, the corresponding pair (n_1, n_2) can be considered as the candidate inter-area buses (i.e. specified boundaries) connected through two oscillating areas. Considering the controlling function (28) as a function of tie-line reactance, the proposed TCSC-based DWADC scheme is developed based on phase angle evaluations from which the corresponding tie-line reactance $\Delta x(t)$ is controlled. In this case, the provided swing formulations (15) are rewritten as follows:

$$M\Delta\ddot{\delta}(t) = L\Delta\delta(t) + g\Delta x(t) \tag{42}$$

where, the parameters g is developed in (n×1) matrix dimension as follows::

$$g = \begin{bmatrix} 0, 0, ..., \beta \\ 0, 0, ..., -\beta \end{bmatrix} \tag{43}$$

In (43), β is a non-zero parameter between $\pm\beta$ values, which is evaluated through the n_1th and n_2th state vectors as $\beta_1=\beta/M_{n1}$ and $\beta_2=\beta/M_{n2}$, respectively. Considering (42) and (43), the corresponding output controlling matrix is provided as follows:

$$\begin{aligned} &C = [C_1\ 0], \\ &C_1 = [0\ 0\ ...\ 1\ 0\ 0\ ...\ -1] \end{aligned} \tag{44}$$

where C_1 is a non-zero parameter is provided through n_1th and n_2th state vectors.

Considering ε_{n1} as non-zero small value through all zero input vectors, the swing mathematical equations (40)-(41) are rewritten as follows:

$$\begin{aligned} &\delta_a \equiv col(\delta_{11}, \delta_{12}, ..., \delta_{1n_1}) \\ &\delta_b \equiv col(\delta_{21}, \delta_{22}, ..., \delta_{2n_2}) \end{aligned} \tag{45}$$

$$\begin{aligned} &\omega_a \equiv col(\omega_{11}, \omega_{12}, ..., \omega_{1n_1}) \\ &\omega_b \equiv col(\omega_{21}, \omega_{22}, ..., \omega_{2n_2}) \end{aligned} \tag{46}$$

Therefore, the corresponding dynamic-state swing mathematical formulations are verified as follows:

$$\begin{bmatrix} \dot{\delta}_a \\ \dot{\delta}_b \\ - \\ \dot{\omega}_a \\ \dot{\omega}_b \end{bmatrix} = \underbrace{\begin{bmatrix} 0 & I \\ L & 0 \end{bmatrix}}_{A} \begin{bmatrix} \delta_a \\ \delta_b \\ - \\ \omega_a \\ \omega_b \end{bmatrix} + \underbrace{\begin{bmatrix} 0 \\ 0 \\ - \\ \beta_1 \varepsilon_{n1} \\ -\beta_2 \varepsilon_{n2} \end{bmatrix}}_{B} \Delta x(t) \tag{47}$$

where ε_{ni} represents an n-dimensional non-zero matrix for all input zero parameters. Also, L represents the Laplacian matrix in an unsymmetrical form which is evaluated as follows:

$$L = \begin{bmatrix} L_1 & L_2 \\ L_3 & L_4 \end{bmatrix}, L_2 = \begin{bmatrix} 0 & 0 \\ 0 & \gamma_{n_1,n_2} \end{bmatrix}_{n_1 \times (n_1+n_2)}, L_3 = \begin{bmatrix} 0 & 0 \\ 0 & \gamma_{n_2,n_1} \end{bmatrix}_{n_2 \times (n_1+n_2)} \tag{48}$$

where, the parameters $\gamma_{n1,n2} \in \mathbb{R}^{1 \times n2}, \gamma_{n2,n1} \in \mathbb{R}^{1 \times n1}$ are defined as:

$$\gamma_{n_1,n_2} = col(0,0,...,\frac{E_{n_1} E_{n_2}}{M_{n_1} x_{n_1,n_2}} \cos(\delta_{n_1 0} - \delta_{n_2 0}))^T \tag{49}$$

$$\gamma_{n_1,n_2} = col(0,0,...,\frac{E_{n_1} E_{n_2}}{M_{n_1} x_{n_1,n_2}} \cos(\delta_{n_1 0} - \delta_{n_2 0}))^T \tag{50}$$

In (49) and (50), the parameters M_{nj}, E_{nj} and δ_{nj0} describe the synchronous machine inertia, internal voltage and phase angle, respectively with respect to pre-fault evaluations through the jth inter-area bus. Also the constant parameter $x_{n1,n2}$ is equal to $x_{n1,n2}= x_{n1,n2}+\Delta x(t_0)$ which represents the corresponding tie-line reactance connected between the two oscillating areas n_1 and n_2.

In (40)-(50), following some mathematical simplifications, it is easily achieved that considering C_B=0 and $C_{AB}\neq$0, the order of test power system provided in Figure 4 is equal to n=2. However, in the real case, following the input signals $\Delta x(t)$ and the corresponding output responses y, there are three dynamic variables which present n=3 as full-order model. It is noted that, following (42), the parameter L represents both the local and inter-area specifications. In this case, by considering the two oscillating areas, the parameter L is included through one inter-area oscillating mode and (n_1+n_2-2) local modes through the reduced-order model. In order to provide proper damping performance of the proposed DWADC scheme, considering specified band-pass filter in the range of inter-area frequency (i.e. 0.1-1 Hz), the corresponding output controlling signals y=(δ_{n1}–δ_{n2}) are provided. In this way, considering some modal analysis evaluations through an offline working mode, the required adjustments are verified. In the case of the provided band-pass filter to be organized as zero-order filter, the corresponding transfer function $G(s)$ of the open-loop power system consists of two oscillating areas,

and TCSC damping controller remains as n=3. Similarity, in the case of reduced-order model, the same results as per *Lemma 1* are obtained.

Lemma 2: Considering $G_r(s)$ as the area transfer functions and TCSC links as the input controlling signals, the phase angle difference between two oscillating areas $\Delta\delta$ is determined as the output controlling signals. In this case, the corresponding transfer function $G_r(s)$ is organized through n=3 as the provided transfer function order.

Proof: Considering $\Delta x(t)$ as a DWADC input signal, the corresponding dynamic state variables of the reduced-order model through EVGs is defined as follows:

$$\underbrace{\begin{bmatrix}\dot{\delta}_a\\ \dot{\delta}_b\\ -\\ \dot{\omega}_a\\ \dot{\omega}_b\end{bmatrix}}_{\dot{\bar{x}}} = \underbrace{\begin{bmatrix}0 & I_{2\times 2}\\ \bar{L} & 0\end{bmatrix}_{4\times 4}}_{A}\begin{bmatrix}\bar{\delta}_a\\ \bar{\delta}_b\\ -\\ \bar{\omega}_a\\ \bar{\omega}_b\end{bmatrix} + \underbrace{\begin{bmatrix}0\\ 0\\ -\\ \gamma\\ -\gamma\end{bmatrix}}_{B}\Delta\bar{x}(t)$$

$$\bar{y} = \underbrace{[1\ \vdots\ 1; 0\ 0]}_{C}\bar{x}, \qquad L = \begin{bmatrix}-\bar{c}_{ab} & \bar{c}_{ab}\\ \bar{c}_{ab} & \bar{c}_{ab}\end{bmatrix} \tag{51}$$

where, the power flow formulation of the provided L matrix consists of c_{ab} parameter that is defined as follows:

$$\bar{c}_{ab} \equiv \frac{\left(E_a E_b \cos(\delta_{a0} - \delta_{b0})\right)}{\bar{x}_{ab} + \Delta\bar{x}(t_0)} \tag{52}$$

In (52), the signs a and b address the two oscillating areas (*Area1* and *Area2*), respectively. It is seen that when considering the two input-output pairs data $\Delta x(t)$-$y(t)$, the corresponding reduced-order model goes to n=2 from which it is concluded that in the case of real system, the relative order goes to n_r=3.

Following *Lemma1* and *Lemma2*, the reduced-order model of the developed virtual system can be defined as a dynamic state model in the form of the following description:

$$\begin{bmatrix}\dot{\bar{x}}\end{bmatrix} = \begin{bmatrix}\bar{A}\end{bmatrix}\bar{x} + \begin{bmatrix}\bar{B}\end{bmatrix}\bar{u}$$
$$\begin{bmatrix}\bar{y}\end{bmatrix} = \begin{bmatrix}\bar{C}\end{bmatrix}\bar{x} \tag{53}$$

In (53), the input variable u is developed in the form of $\bar{u} = K\,\bar{x}(t) \square\ r(t)$ where considering the closed loop state feedback structure from the input signal u to the output response y(t), a proper dynamic performance can be found. In this case, considering the developed state feedback, the construction of the dynamic state variables through the provided reduced-order model (31) is defined as follows:

$$\delta(t) = \angle(\tilde{V}_{b1}(t) + jx_{a1}\tilde{I}(t)) - \angle(\tilde{V}_{b2}(t) - jx_{a2}\tilde{I}(t)) \tag{54}$$

where, V_{b1} and V_{b2} represent the voltages magnitudes through inter-area with respect to the specified oscillating areas. Also, *I* represents the inter-area tie-line current through oscillating areas. Finally, the state variables of a realistic full-order model can be defined through the following form:

$$\begin{aligned} \left[\dot{x}\right] &= [A]x + [B]u \\ [y] &= [C]x \\ [y_m](t) &= \left[G_{(s)}\right][y](t) \end{aligned} \tag{55}$$

In (55), $G(s)$ represents a zero filter function through the corresponding order developed from Hurwitz-based zero dynamics. Considering the input state variables *u*, the closed loop controlling signals are limited with the output variables $y_m(t)$ that follow $\bar{y}(t)$ properly through continuous time durations. Based on this, the following assumptions have been adopted.

-Assumption1: Considering $G_p(s) = k_p\left(Z_p(s)/P_p(s)\right) = G(s)[C(sI - A)^{-1}Bu](t)$, it is assumed that, the polynomial function Z(s) includes the left-side eigenvalues.

-Assumption2: There are n=4 as the pole order $P_p(s)$ which is fixed during dynamic evaluations.

-Assumption3: The gain factor k_p is specified based on the high frequency ratio and fixed.

-Assumption4: The order of the transfer function $G_m(s) \square [\bar{C}(sI - \bar{A})^{-1}\bar{B}r](t)$ is the same as $G_p(s)$ order provided in Assumtion4 which is equal to n=2.

Considering Hurwitz-based theory and with respect to the abovementioned assumptions, the wide-area input signals *u(t)* can be modelled with the model-reference controller [31] as follows:

$$u(t) = \theta_1^T v_1(t) + \theta_2^T v_2(t) + \theta_{20} y_m(t) + \theta_3 r(t) \tag{56}$$

where, θ_i represents some specific values with respect to the inter-area oscillation damping ratio.

In (56), v_1 and v_2 are the two corresponding filtering variables which are defined as follows:

$$v_1(t) = \frac{q(s)}{\Lambda(s)}[u](t) \tag{57}$$

$$v_2(t) = \frac{q(s)}{\Lambda(s)}[y](t) \tag{58}$$

where, $\Lambda(s)$ presents the Hurwitz polynomial function with n=3 mathematical order as $\Lambda(s)$=k_0+k_1s+k_2s^2. Also, $q(s)$ is the second-order n=2 Laplacian function $q(s)=[1,s,s^2]$ following v_1, $v_2 \in \Re^3$ and $v_{20} \in \Re$.

Considering the model reference control (MRC) mathematical theory, two provided filtering parameters v_1 and v_2 and can be rewritten as follows:

$$\dot{v}_1(t) = A_\lambda v_1(t) + B_\lambda u(t) \tag{59}$$

$$\dot{v}_2(t) = A_\lambda v_2(t) + B_\lambda u(t) \tag{60}$$

In (59) and (60), A_λ and B_λ are the Laplacian and input coefficient matrices respectively. They are defined as follows:

$$A_\lambda = \begin{bmatrix} 0 & 1 & 0 \\ 0 & 0 & 1 \\ -\kappa_0 & -\kappa_1 & -\kappa_2 \end{bmatrix} \times \begin{bmatrix} 1 \\ s \\ s^2 \end{bmatrix} \tag{61}$$

$$B_\lambda = \begin{bmatrix} 0 \\ 0 \\ 1 \end{bmatrix} \tag{62}$$

Finally, the following constant parameters θ_1, θ_2, θ_{20} and θ_3 and based on Diophantyne mathematical formulation provided in [18], the input controlling function (56) is solved in the form of Laplacian functions as follows:

$$\begin{aligned} &\left(\theta_1^T q(s)\right) P_p(s) + \left(\theta_2^T q(s) + \theta_{20}\Lambda(s)\right) k_p Z_p(s) \\ &= \Lambda(s)\left(P_p(s) - k_p \theta_3 Z_p(s) P_m(s)\right) \end{aligned} \tag{63}$$

where, $P_m(s)$ is a polynomial function with respect to the dynamic state model provided in (53).

5. Simulation Results

In this section, the effectiveness of the proposed DWADC strategy is investigated with a practical case study of Iran National Power Grid. The Single line diagram (SLD) of the "North Practical Power Grid" is illustrated in Figure 5.

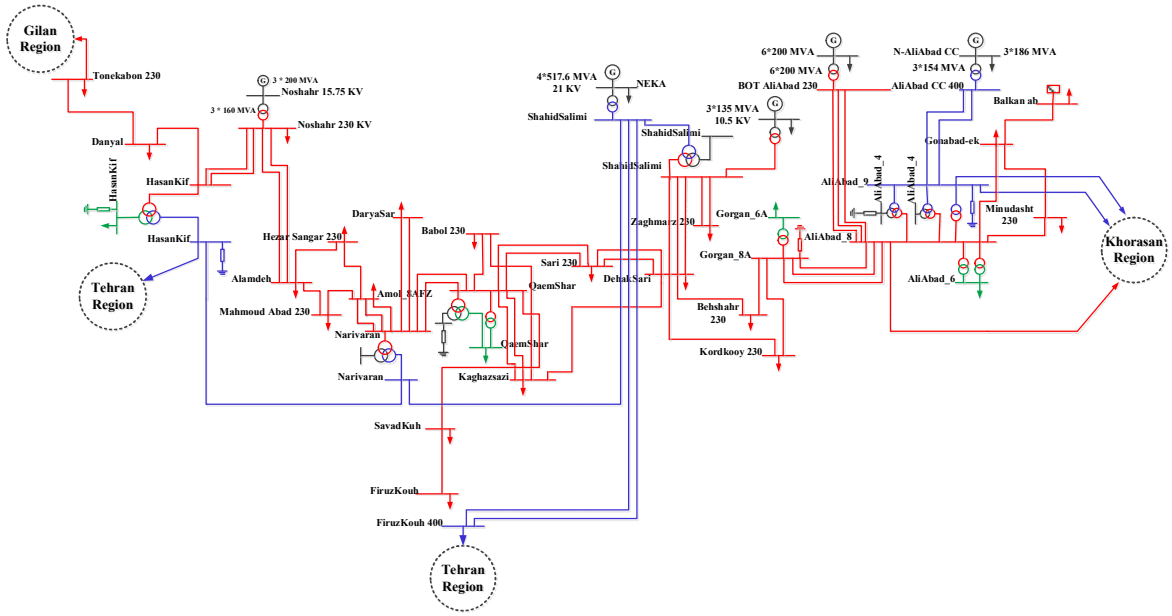

Figure 5: North IRAN national power grid

From Figure 5, The Iran national power grid includes four different regions that are Gilan, Khorasan, Tehran and Mazandaran. The national power grid consists of several synchronous generators and tie-lines. Generally, the system has about 450 synchronous machines which generate 63384 MW of power with different generation technologies (i.e. steam, gas, combined cycle, hydro and renewable energy sources). The system generators are equipped with PSSs which are implemented individually for damping local modes and provide some damping performances with respect to the inter-area oscillations. Also, there are a set of buses equipped with PMUs to measure the wide areas' signals using the WAMS technology. **(R1-C5)**In this case, based on the proposed WADC scheme, it is considered that all generators terminals are equipped with PMU devices which measure the voltage and current phasors through consecutive time moving windows.

Evaluating the eigenvalues showed that the system has a potential of inter-area oscillations throughout different regions. In this case, following different simulation studies, the performance of the proposed DWADC controller with respect to the provided oscillating areas is evaluated. Based on Figure 5, considering 3-*ph* short circuit fault event at bus *ShahidSalimi* and tripping two tie-lines connected between buses *ShahidSalimi* and *Firozkouh400*, the system dynamic behaviors are investigated. In this case, considering the proposed reduced-order model, the power grid can be developed through two oscillating areas with $n_1=n_2=8$ as the order of the system. The generator parameters of the reduced-order model consist of P_{mi}=1 p.u., E_i=1 p.u., and line reactance area x_{ij}=0.1 p.u. for all internal lines. Also, through the reduced order model, the tie-line reactance through the oscillating areas are considered 100 times higher than the interconnected lines. Conducting a modal analysis through the reduced-order model indicates that the system can be reduced through sixteen conjugate eigenvalues

(EIGs) which can be identified using roots' specifications as presented in Table 1.

(R1-C6)Table 1: Modal analysis results with respect to reduced-order model

Mode Num.	EIG Real Part	Freq.	Mode Num.	EIG Real Part	Freq.
Mode01	0	0	Mode07	-0.0332	2.477
Mode02	-0.7026	3.234	Mode08	-0.638	2.8885
Mode03	-0.09649	1.781	Mode09	-0.555	3.375
Mode04	-0.0957	1.201	Mode10	-0.511	2.236
Mode05	-2.000	2.349	**Mode11**	**+0.0212**	**0.668**
Mode06	-1.0009	0.652	Mode12	-0.711	3.564

From Table 1, it is clear that the *Mode1* is related to a DC mode (i.e. the summation of Laplacian matrix rows are nonzero). Also, the modal analysis evaluations indicate that there are two inter-area modes including *Mode07* and the *Mode11* which represent the corresponding two oscillating areas. In this case, *Mode11* with the damping ratio *DR*=+0212 represents an unstable inter-area oscillation through the oscillating Areas (*Area1* and *Area2*). From Table 1, there are ten eigenvalues *Mode01-05,07-10* and *12* which develop the local modes corresponding to the synchronous generators' models. In the case of the open loop model, without considering the corresponding damping factor *D* (6), the damping ratios for all identified local and inter-area modes clearly go to zero. In order to provide the unstable inter-area mode, following DWADC scheme, a 2^{nd} order band pass filter is designed with a bandwidth frequency of f_s=0.1-0.9 Hz. In this case, the bandwidth filter is provided through the phase angle difference $\Delta\delta$ of oscillating areas EVG1 and EVG2 from which oscillations in the range of inter-area frequency is obtained. The phase angle and speed deviations of synchronous generators through the two oscillating areas (*Area1* and *Area2*), without considering the proposed DWADC scheme and the corresponding bandwidth filters, are shown in Figure 6.

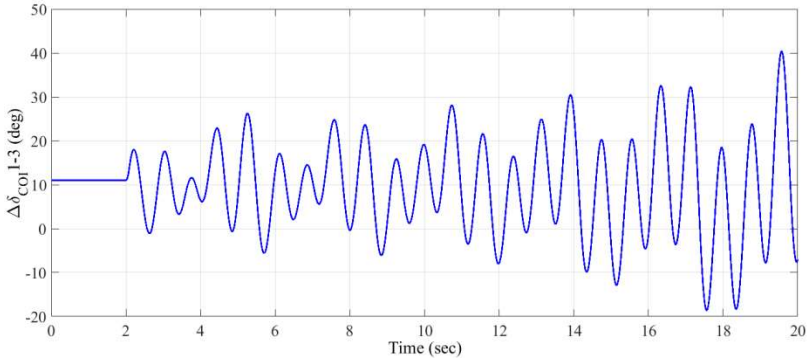

(a) Phase angle differences through oscillating generators G_1 and G_3

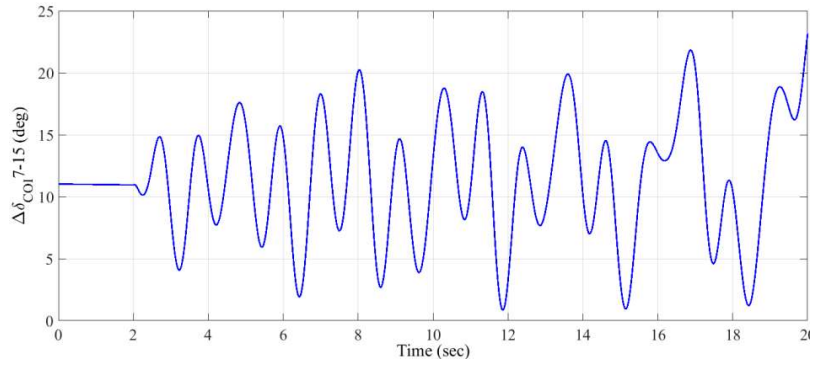

(b) Phase angle differences through oscillating generators G_7 and G15

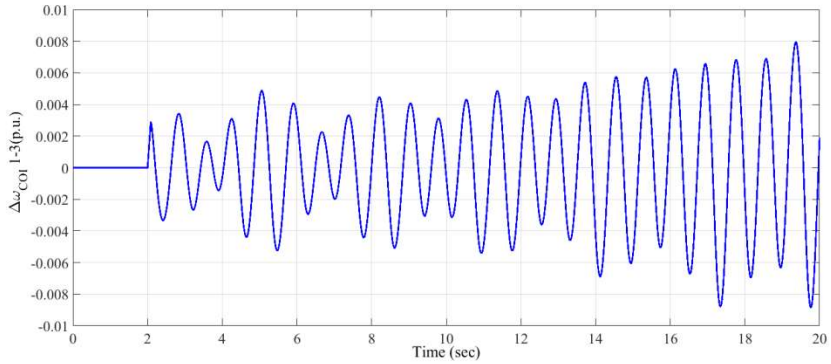

(c) Inter-area speed deviation through oscillating generators G_1 and G_3

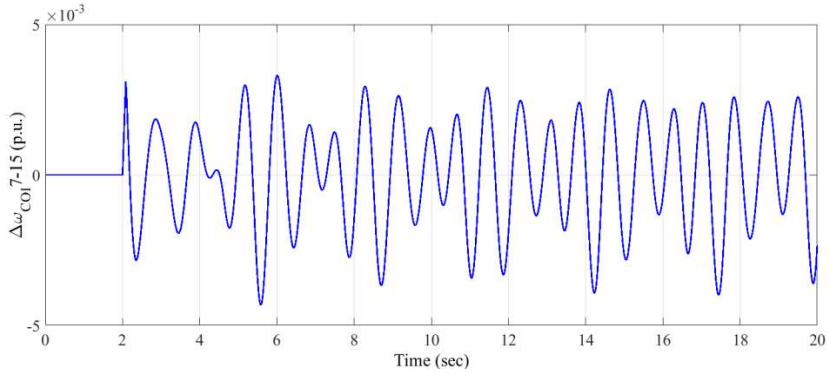

(d) Inter-area speed deviation through oscillating generators G_7 and G15

Figure 6: The speed and phase angle oscillations through two oscillating areas

As it can be seen in Figure 6, without developing the DWADC scheme, generators oscillate together through a negative damping ratio. Also, it is shown that, without considering provided filters, the corresponding output signals include different variations through both local and inter-area frequencies. In this case, considering provided bandwidth filters, the dynamic state variations are evaluated. Figure 7 represents the output band-pass filter (BPF) signal through dynamic oscillations of two oscillating areas.

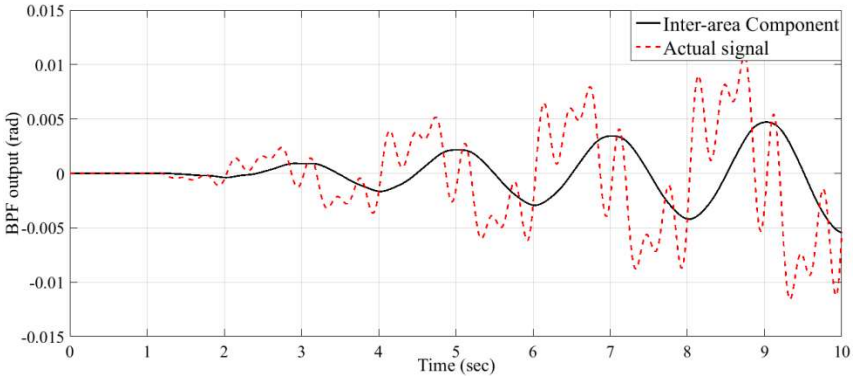

(a)

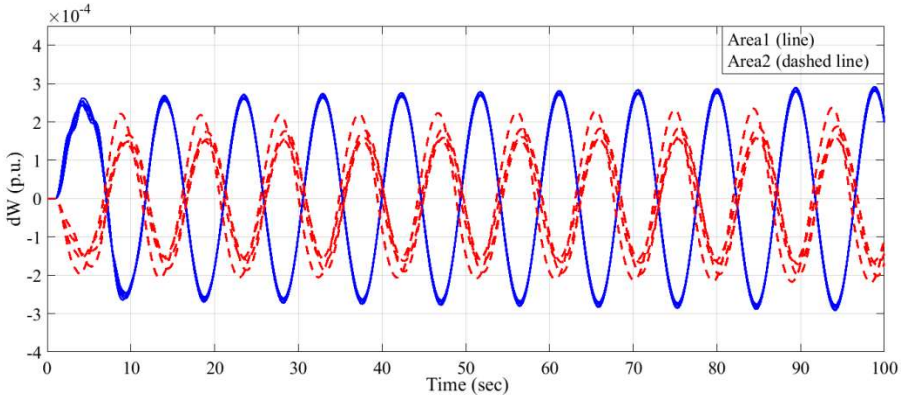

(b)

Figure 7. Inter-area speed oscillations extracted from BPF and ERA techniques.

(a) The output of BPF filter for a full-order model vs reduced-order equivalent system.

(b) Inter-area speed deviation through two oscillating areas extracted by ERA algorithm

From Figure 7, it is illustrated that, considering a BPF filter, the proper output signals in the range of inter-area oscillations are provided. It is worth noting that, in real case, some modal decomposition techniques as Eigenvalue Realization Algorithm (ERA) or other similar strategies are applied for filtering the PMU oscillating signals, which depend on the estimated frequency components, and signals through inter-area frequencies. In a comparative case, the inter-area speed oscillations of the synchronous machines extracted by the ERA algorithm are shown in Figure 7(b).

From Figure 7(b), considering the reduced-order inter-area model presented in in Sec.3, the power system can be presented through two equivalent virtual generators *EVG1* and *EVG2* presenting two oscillating areas. In this case, considering the TSCS between the two oscillating areas (*Area1* and *Area2*) and following the damping index D as a DWADC feedback controlling block, the controller damping performance is investigated. To do this, the provided damping index D is increased through two different steps 20% and 50% from the initial condition. In order to provide the best DWADC damping performance, considering the inter-area phase angle deviation $\Delta\delta$ through the two oscillating areas and applying the MRC model (55)-(61) as a damping controller,

the closed-loop response of the provided controlling model is evaluated. In this case, the corresponding controlling parameters k_0 , k_1 and k_2 provided in (60) are adjusted optimally with which the full-order system responses track the input dynamic variables properly. Figure 8 represents the inter-area phase angle and speed deviations through two oscillating areas with respect to different controlling gains k_1, $k2$ and k_3.

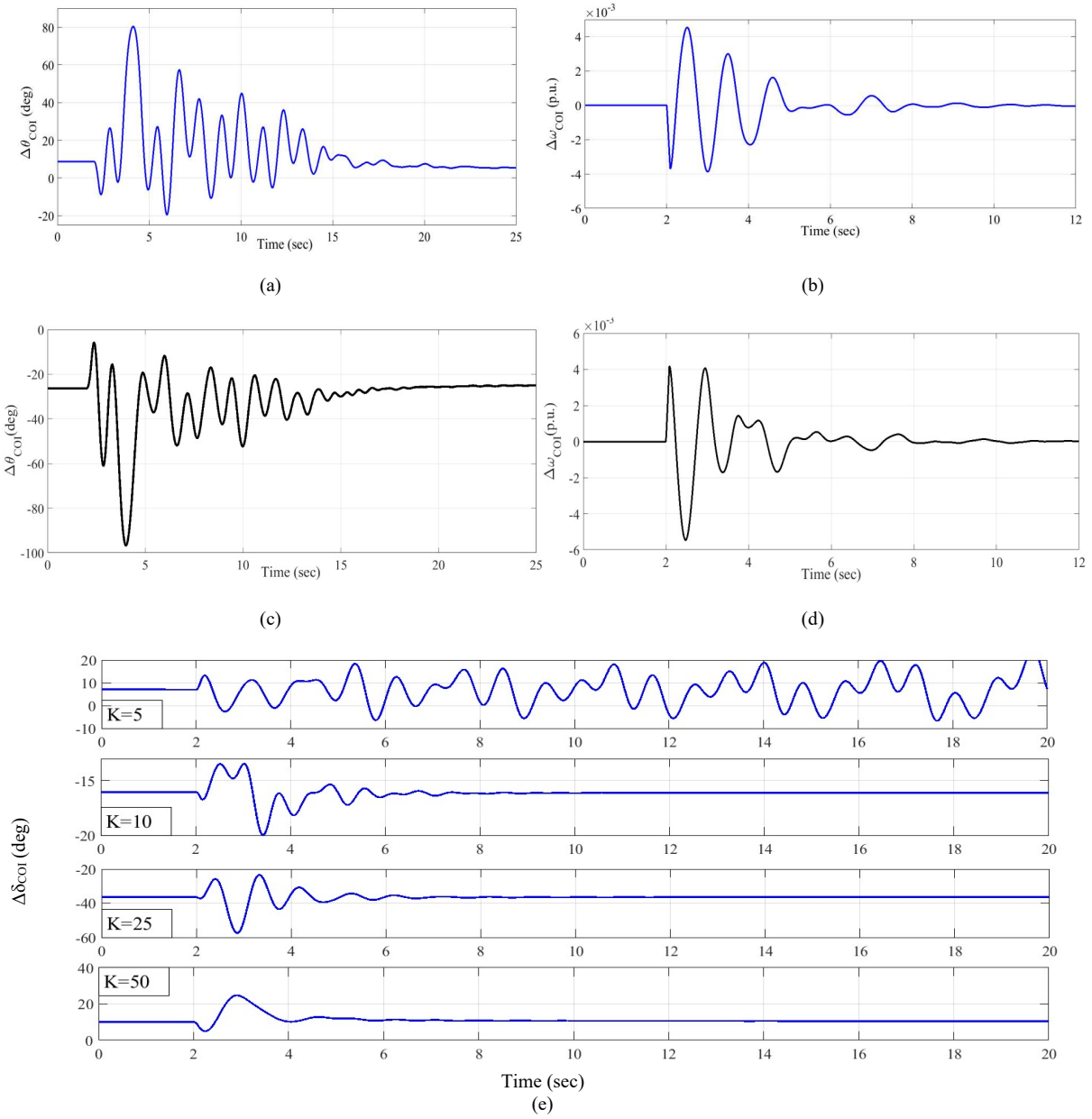

Figure 8: DWADC damping performance considering TCSC links with respect to controlling gains.

(a) Inter-area rotor angle deviations with respect to damping factor D=20%, (b) Inter-area speed deviations with respect to damping factor D=20%, (c) Inter-area rotor angle deviations with respect to damping factor D=50%, (d) Inter-area speed deviations with respect to damping factor D=50%, (e) Rotor angle dynamic oscillation two oscillating with respect to different values K.

In order to evaluate the damping performance of the proposed DWADC controller, considering different controlling gains, the provided damping ratios are investigated. In this case, with respect to provided inter-area mode specifications, the feedback controlling gains are adjusted optimally. The inter-area phase angle and speed

deviations with respect to the controlling gains K are shown in Figure 8(e). It is illustrated that increasing the controlling gain K improves the system damping performance with K=50 provides the best damping performance with the proper damping ratio.

(R1-C7) From Figure 8(e), it is illustrated that, considering feedback controlling gains, there are different dynamic responses through several damping ratios. In order to evaluate the signal damping ratio and settling time, by using the eigenvalue analysis through nominated oscillatory mode, the corresponding parameters can be achieved. Through real-time evaluations, it is resulted that considering controlling gains $K1$=5, $K2$=10, $K3$=25 and $K4$=50 the signal damping ratios (DR) are evaluated as $DR1$=-0.025, $DR2$=+0.2, $DR3$=+0.3 and $DR4$=+0.4 which are corresponded with settling times (STs), $ST1$=∞, $ST2$=5s, $ST3$=3s and $ST4$=1s for damping the inter-area oscillations.

In fact, the provided central controller shifts the real part of inter-area modes, which provides the proper damping performance through the reduced-order system. The developed DWADC controller is equipped with simple feedback controllers which do not have the required intermediate decomposition steps as applied through MRC technique. Therefore, it prevents considerable delays through the dynamic response of damping controller which provides the proper settling time. Also, comparing DWAC damping performance with the developed MRC technique, the proposed DWADC closed-loop controller provides better damping performance so that the dynamic oscillations are damped properly within a relatively short time duration with respect to the MRC technique.

It is worth noting that, in the case of fixed controlling model, when the controlling parameters are varied during time windows, a self-adjusting adaptive DWADC scheme is more proper as a controlling scheme for a real-time working mode. However, the base controlling model and the corresponding damping factors provide an adequate damping performance with respect to different oscillating modes.

6. Conclusions

In this paper a TCSC-based wide-area damping controller has been proposed for damping inter-area oscillations through bulk power systems. For this issue, at each time window, the PMU signals are gathered simultaneously adopting an online non-model-based procedure, the oscillating areas are identified. In the case of identifying unstable inter-area oscillations, the proposed DWADC scheme is activated for evaluating system dynamic state variables, and finding proper damping ratios. By monitoring a closed-loop damping performance, the order of bulk power systems is reduced and the base controlling model is designed.

The proposed DWADC scheme consists of specific filtering and controlling blocks for which, with respect to inter-area mode specifications, the online parameters are adjusted optimally. It is noted that the proposed controlling structure is a deduction of an inter-area modeling structure from which considering TCSC links between two oscillating areas, the inter-area controlling model is provided.

In order to evaluate the effectiveness of the DWADC scheme, considering a practical case study from Iran National Power Grid, a reduction-order model has been developed with which, by decreasing the system size and complexity, DWADC dynamic behaviors have been investigated. A distributed concept of the damping controller has been developed, for which depending on the PMU measurements, the controlling model and corresponding proper responses are achieved.

Simulation results show that the proposed controller provides proper damping performances thorough high damping ratios and therefore can be implemented in a real-life testbed that consists of different oscillating areas. Also, numerical results indicate that the proposed reduced-order technique is a useful tool for reducing a large-scale power system with a simpler model which significantly helps to identify the main problem and to design an associated controlling model utilizing less mathematical formulations.

References

[1] Ranjbar, S., Aghamohammadi, M., Haghjoo, F., 'A new scheme of WADC for damping inter-area oscillation based on CART technique and Thevenine impedance', Electrical Power and Energy Systems, 2018, 94, pp. 339–353.

[2] Y. Liu et al., "A US-wide power systems frequency monitoring network," in Proc. IEEE PES General Meeting, Jun. 2006, pp. 1914–1921.

[3] Sarkar M, Subudhi B. Fixed low-order synchronized and non-synchronized wide-area damping controllers for inter-area oscillation in power system. Int J Electric Power Energy Syst 2019;113:582-596.

[4] Mohamad Javad Alinezhad, Masoud Radmehr and Soheil Ranjbar, "Adaptive Wide Area Damping Controller for Damping Inter-Area Oscillations Considering High Penetration of Wind Farms, International Transactions on Electrical Energy Systems, March 2020. http://dx.doi.org/10.1002/2050-7038.12392.

[5] Ranjbar, S., Aghamohammadi, M., Haghjoo, F., 'Determining Wide Area Damping Control Signal (WADCS) Based on C5.0 Classifier', 24th Iranian Conference on Electrical Engineering (ICEE), May 2016, Shiraz ,Iran.

[6] Liao K, Xu Y, Zhou H. A robust damping controller for DFIG based on variable-gain sliding mode and Kalman filter disturbance observer. Int J Electric Power Energy Syst 2019;107:569-576.

[7] A. R. Messina, V. Vittal, D. Ruiz-Vega, and G. Enriquez-Harper, "Interpretation and visualization of wide-area PMU measurements using Hilbert analysis," IEEE Trans. Power Syst., vol. 21, no. 4, pp. 1760–1771, 2006.

[8] Noori A, Shahbazadeh MJ, Eslami M. Designing of wide-area damping controller for stability improvement in a large-scale power system in presence of wind farms and SMES compensator. Int J Electric Power Energy Syst 2020.

[9] G. Tao, Adaptive Control Analysis Design and Analysis. Hoboken, NJ: Wiley Interscience, 2003.

[10] Ranjbar, S., Aghamohammadi, M., Haghjoo, F., 'Damping inter-area Oscillation in Power System by Using Global Control Signals based on PSS devices', 25th Iranian Conference on Electrical Engineering (ICEE), May 2017, Tehran, Iran.

[11] R. Emami and A. Abur, "Reliable placement of synchronized phasor measurements on network branches," in Proc. IEEE PSCE, Seattle, WA, Mar. 15–19, 2009, pp. 38–43.

[12] Javed R, Mustafa G, Khan AQ, Abid M. Networked control of a power system: A non-uniform sampling approach. Electr Power Syst Res 2018;161:224-235.

[13] Li M, Chen Y. A wide-area dynamic damping controller based on robust H1control for wide-area power systems with random delay and packet dropout. IEEE Trans Power Syst 2018;33(4):4026-4037.

[14] C. W. Taylor, D. C. Erickson, K. E. Martin, R. W. Wilson, and V. Venkatasubramanian, "WACS—wide-area stability and voltage con-trol system: R & D and online demonstration," Proc. IEEE, vol. 93, no. 5, pp. 892–906, May 2005.

[15] Duan JJ, Xu H, Liu W. Q-learning based damping control of wide-area power systems under cyber uncertainties. IEEE Trans Smart Grid 2018;9(6):6408-6418.

[16] Masoud Rezaee, Mahmoud Samiei Moghadam, Soheil Ranjbar, "Online estimation of power system separation as controlled islanding scheme in the presence of inter-area oscillations," Sustainable Energy, Grids and Networks, vol.21, Feb 2020.

[17] Amraee, T., Ranjbar, S. 'Transient instability prediction using decision tree technique', IEEE Trans. Power Syst., 2013, 28, (3), pp. 3028-3037.

[18] Simon L, Swarup KS, Ravishankar J. Wide area oscillation damping controller for DFIG using WAMS with delay compensation. IET Renewable Power Gener 2019;13(1):128-137.

[19] Liu M, Dassios I, Tzounas G, Milano F. Stability analysis of power systems with inclusion of realistic-modelingWAMS delays. IEEE Trans Power Syst 2019;34(1):627-636.

[20] Ranjbar, S., Aghamohammadi, M., Haghjoo, F., 'Real Time Transient Instability Assessment Based-on Bayesian Theory', 23th Iranian Conference on Electrical Engineering (ICEE), May 2015, Tehran, Iran.

[21] PNNL EIOC [Online]. Available: http://eioc.pnl.gov/research/gridsta-bility.stm

[22] S. Arabi, H. Hamadanizadeh, and B. Fardanesh, "CSC performance studies on the NY state transmission system," IEEE Trans. Power Syst., vol. 17, no. 3, pp. 701–706, Jun. 2002.

[23] B. Chaudhuri and B. C. Pal, "Robust damping of multiple swing modes employing global stabilizing signals with a TCSC," IEEE Trans. Power Syst., vol. 19, no. 1, pp. 499–506, Feb. 2004.

[24] Ranjbar, S., Aghamohammadi, M., Haghjoo, F., 'Real Time Wide Area Damping Control Signal to Damp Inter-Area Oscillation In Power System', 25th Iranian Conference on Electrical Engineering (ICEE), May 2017, Tehran, Iran.

[25] Prakash T, Singh VP, Mohanty SR. A synchrophasor measurement based wide-area power system stabilizer design for inter-area oscillation damping considering variable time-delays. Int J Electric Power Energy Syst 2019;105:131-141.

[26] Soheil Ranjbar, Mohammad Reza Aghamohammadi “A New Method for Transient Instability Detection of Wide Area Network Based-on SVM Theory”, 29st International Power System Conference 2014 (PSC 2014), 27-28 Oct 2014, Tehran, Iran.

[27] Padhy B. Adaptive latency compensator considering packet drop and packet disorder for wide area damping control design. Int J Electric Power Energy Syst 2019;106:477-487.

[28] Ranjbar, S., Aghamohammadi, M., Haghjoo, F., ‘Adaptive Wide Area Damping Controller for Damping Inter-Area Oscillations On Power System’, 24th Iranian Conference on Electrical Engineering (ICEE), May 2016, Shiraz, Iran.

[29] A. Chakrabortty, J. H. Chow, and A. Salazar, “A measurement-based framework for dynamic equivalencing of power systems using wide-area phasor measurements,” IEEE Trans. Smart Grid, vol. 1, no. 2, pp. 68–81, Mar. 2011.

[30] A. Chakrabortty, “Wide-Area Damping Control of Large Power Systems Using a Model Reference Approach,” in Proc. 50th IEEE Conf. Decision Contr., FL, 2011, pp. 2189–2194.

[31] Iman Sepehrirad, Reza Ebrahimi, Esmaeil Alibeiki, Soheil Ranjbar, " Intelligent Differential Protection Scheme for Controlled Islanding of Microgrids based on Decision Tree Technique", Journal of Control, Automation and Electrical Systems(JCAE), April 2020.DOI:10.1007/s40313-020-00588-7